Theoretical Study on Spectroscopic Properties of Positive, Neutral, and Negative Species of BCl_2 and $AlCl_2$: The Stability of the Negative Species

Kyoung K. Baeck*,† **and Heechol Choi**

Department of Chemistry, Kang-Nung University, Kang-Nung, 210-702, Korea

Suehiro Iwata‡

Institute for Molecular Science, Okazaki, Aichi 444-8585, Japan

Received: March 29, 1999; In Final Form: June 4, 1999

Accurate and predictive values of the bond lengths and angles, dipole moments, and vibrational frequencies of $BCl_2^+(X^1\Sigma_g^+)$, $BCl_2(\tilde{X}^2A_1)$, and $BCl_2^-(\tilde{X}^1A_1, \tilde{a}^3B_1)$ and the corresponding aluminum analogs are calculated by Becke's three-parameter density-functional-theory (B3LYP) method with the augmented correlation consistent triple- and quadruple-ζ (aug-cc-pVTZ and aug-cc-pVQZ, respectively) basis sets. The coupled-cluster singles, doubles, and noniterative triples (CCSD(T)) method employing the aug-cc-pVTZ basis set is also used to augment the B3LYP results. The ionization energies and electron affinities are also calculated by the B3LYP/aug-cc-pV5Z method at the B3LYP/aug-cc-pVQZ geometry and the CCSD(T)/aug-cc-PVQZ method at the CCSD(T)/aug-cc-pVTZ geometry, as well as by the G1, G2, CBS-4, and CBS-Q methods. It is shown that the negatively charged species, which have never been studied experimentally, are stable both in singlet and triplet spin tates with electron diffinities of 1.40 eV/0.25 eV and 2.37 eV/0.46 eV for singlet-triplet states of BCl_2^- and $AlCl_2^-$, respectively. The photoelectron spectra for the electron detachment of the anions are simulated by calculating the Franck−Condon factors. The photoelectron spectra for the singlet and triplet states of BCl_2^- turn out to be very similar to $AlCl_2^-$ analogs. While the photoelectron spectra for $\tilde{X}^2A_1(MCl_2) \leftarrow \tilde{X}^1A_1(MCl_2^-)$, M = B and Al, have complicated combination bands, those for $\tilde{X}^2A_1(MCl_2) \leftarrow \tilde{a}^3B_1(MCl_2^-)$, M = B and Al, have only one vibrational progression of the symmetric stretch mode.

Introduction

The boron chlorides are widely used in the commercial plasma etching of metals and semiconductors.[1] Many experimental and theoretical works are being conducted to elucidate the underlying mechanisms and to model the overall plasma processes.[2] Such works demand reliable information on physical and chemical properties of chemical species involved in the processes: the information regarding molecular geometries, vibrational properties, and energetic properties (such as ionization energies (IE) and electron affinities (AE)) is the most basic prerequisite for other subsequent experimental and theoretical analyses.

Basic properties of BCl_3, BCl_3^+, and BCl_3^- have been studied quite intensively in recent experimental and theoretical works.[3−5] On the other hand, only a few experimental data[3,5,6] for BCl_2 and BCl_2^+ are available, and a recent theoretical study[7] only reports data for BCl_2 and BCl_2^+. The properties of BCl_2^- have not been studied either experimentally or theoretically, so far. Because BCl_2 and its ions are expected to play a role as active transients or intermediates in the overall plasma processes, information regarding their spectroscopic and energetic properties is among the most urgently required in this research area.

In the present work, we have used the most highly sophisticated theoretical methods applicable on these systems, i.e., Becke's three-parameter hybrid density-functional-theory (B3LYP) method[8] and the coupled-cluster singles, doubles, and noniterative triples (CCSD(T)) method[9] in conjunction with aug-cc-pVTZ and aug-cc-pVQZ basis sets. The geometries and spectroscopic properties of the lowest singlet and triplet states of BCl_2^- as well as those of the ground states of BCl_2 and BCl_2^+ are calculated, and the photoelectron spectra of two states of the negative ions are simulated by calculating the Franck−Condon factors.

The corresponding information for isovalent $AlCl_2$, $AlCl_2^+$, and $AlCl_2^-$ is also calculated because they are also expected to be involved in the commercial etching processes of aluminum containing substrates.[1,10] These aluminum dichlorides have attracted little attention and only an ESR study[11] on $AlCl_2$ and a theoretical study[12] using the MBPT(2) method for the geometry of $AlCl_2^+$ and $AlCl_2$ have been reported recently. The vibrational properties of $AlCl_2^+$ and $AlCl_2$ and anything regarding $AlCl_2^-$, either theoretically or experimentally, have not been reported.

We expect our present work to provide useful and reliable information for BCl_2^-, $AlCl_2^+$, $AlCl_2$, and $AlCl_2^-$, and it could initiate further theoretical and experimental work related to these chemical species.

Computational Details

Throughout this work, the Gaussian94 program package[13] is used for all calculations with the B3LYP method,[8] the G1 and G2 theoretical methods,[14] and the complete basis set limit (CBS-4 and CBS-Q) methods.[15] On the other hand, the ACES-

---

† Corresponding author. E-mail address: baeck@chem.kangnung.ac.kr.
‡ E-mail address: iwata@ims.ac.jp.

10.1021/jp991072j CCC: $18.00

TABLE 1: Bond Lengths (R_e, Å), Bond Angles (∠, degree), Dipole Moments(μ, debye), Vibrational Frequencies(ν, cm^{-1}), and IR Intensities(I, km mol^{-1}) of the Positive ($X\Sigma_g^{1+}$), the Neutral ($\tilde{X}^2A_1$), and the Negative ($\tilde{X}^1A_1$ and $\tilde{a}^3B_1$) States of BCl_2 Systems

method	R_e	∠	μ	$\nu_1(I_1)$	$\nu_2(I_2)$	$\nu_3(I_3)$
$BCl_2^+(X\Sigma_g^{1+})$						
(CCSD(T)/6-311G(2d))[a]	1.620	180	0	553(0)	324	1420
(CCSD(T)/6-311G(2df))[b]	1.616	180	0	566(0)	334	1464
CCSD(T)/aug-cc-pVTZ	1.621	180	0	561(0)	326(30)	1451(582)
(B3LYP/cc-pVTZ)[a]	1.616	180	0	560(0)	326(15)	1450(553)
B3LYP/aug-cc-pVTZ	1.616	180	0	560(0)	327(28)	1448(544)
B3LYP/aug-cc-pVQZ	1.614	180	0	560(0)	326(28)	1447(546)
exptl					325 ± 15[c]	1436[d]
$BCl_2(\tilde{X}^2A_1)$						
(CCSD(T)/cc-pVTZ)[a]	1.737	125.3		693	288	956
CCSD(T)/aug-cc-pVTZ	1.732	125.3	0.23	698(21)	281(1)	987(391)
(B3LYP/cc-pVTZ)[a]	1.731	125.6		685(22)	281(1)	964(389)
B3LYP/aug-cc-pVTZ	1.731	125.7	0.23	681(19)	281(1)	963(389)
B3LYP/aug-cc-pVQZ	1.728	125.8	0.24	680(19)	282(1)	964(387)
exptl				731[e]		976,[d]966[e]
$BCl_2^-(\tilde{X}^1A_1)$						
CCSD(T)/aug-cc-pVTZ	1.916	103.5	2.84	519(94)	248(5)	492(307)
B3LYP(aug/cc-pVTZ	1.921	104.1	2.93	497(77)	239(7)	457(303)
B3LYP/aug-cc-pVQZ	1.915	104.3	2.95	498(73)	241(6)	464(300)
$BCl_2^-(\tilde{a}^3B_1)$						
CCSD(T)/aug-cc-pVTZ	1.849	118.9	1.82	574(14)	227(1)	722 [f](188)
B3LYP/aug-cc-pVTZ	1.848	120.1	1.96	544(22)	224(3)	690(199)
B3LYP/aug-cc-pVQZ	1.842	120.3	2.02	544(28)	226(4)	697(191)

[a] The results by Warschkow and co-workers.[7] [b] The results by Jacox and co-workers.[3] [c] From the dispersed emission spectrum.[5] [d] The experimental result from IR spectra after the interaction of excited neon atoms with BCl_3.[3] [e] The experimental values from IR spectra after radiolysis and photolysis of BCl_3.[6] [f] This value may possibly be affected by symmetry breaking.

II program package[16] is used for all calculations with the CCSD(T) method.[9] All electrons are included in the B3LYP calculations for geometry optimizations and vibrational properties, but valence electrons only are correlated in the corresponding CCSD(T) calculations by the drop-MO analytic gradient method[17] implemented in the ACES-II program package by one of the present authors (K.K.B.). The calculations for open-shell states are performed by using the unrestricted Hartree−Fock reference orbitals, and the possibility of spin contamination is carefully guarded against.

According to the previous study[7] on BCl_2 and BCl_2^+, the vibrational frequencies from the CCSD(T)/cc-pVTZ method were closer to those from the B3LYP/cc-pVTZ method rather than those from the BLYP/cc-pVTZ method, and this fact is one of the reasons for the selection of the B3LYP functional in this work. These two highly reliable and complementary theoretical methods, i.e., the B3LYP and the CCSD(T) methods, in conjunction with very large basis sets are used as the main computational tools in this work.

To make a systematic approach toward the near-basis-set-limit results for systems including negative ions, the augmented correlation-consistent polarized valence *n*-triple ζ basis sets, aug-cc-pVXZ,[18] are employed here. The aug-cc-pVDZ, the aug-cc-pVTZ, the aug-cc-pVQZ, and the aug-cc-pV5Z basis sets are used without any modification in the B3LYP calculations. On the other hand, the CCSD(T) calculations are carried out by using slightly modified aug-cc-pVTZ basis sets. The modification is made by using the general linear transformation proposed by Davidson[19] to remove the linear dependencies and to make the size of basis smaller without detriment to the accuracy of the final results. According to the procedure, the modified aug-cc-pVTZ basis sets with (13+3,7+3,3,2)/[3+3,2+3,3,2] contraction for the Cl atom and (8+3,3+3,3,2)/[2+3,1+3,3,2] contraction for the B atom are derived from the original aug-cc-pVTZ basis sets. This modification is required to employ the efficient analytic energy gradient of the CCSD(T) method. The effects of the modification are checked by a few separate calculations, and it turned out to be less than 10^{-8} hartree in energy, while vibrational properties were completely unaffected within the numerical accuracy of calculations.

All the other aspects of the calculations are straightforward in accordance with the well-established procedures used in the Gaussian94 and ACES-II program packages.

The photoelectron spectra of singlet and triplet states of anions are simulated by calculating the Franck−Condon factors (FCF) within the harmonic approximation and the Condon approximation. The procedure we applied for the calculations of the FCF is based on the ideas proposed by Sharp and Rosenstock,[20] implemented in computer codes by Momose and co-workers,[21] and modified to facilitate its use by one of the present authors (S.I.).

Results and Discussions

Geometries and Vibrations. The bond lengths and angles of the ground electronic states of positive ions ($X\Sigma_g^{1+}$ state of BCl_2^+ and $AlCl_2^+$), neutrals ($\tilde{X}^2A_1$ state of BCl_2 and $AlCl_2$), and the lowest singlet and triplet states of negative ions ($\tilde{X}^1A_1$ and $\tilde{a}^3B_1$ states of BCl_2^- and $AlCl_2^-$) are optimized using the B3LYP method with the aug-cc-pVTZ and the aug-cc-pVQZ basis set, and the results are given in Tables 1 and 2. The dipole moments, harmonic frequencies, and IR intensities are calculated at the optimized geometry by the same method used for the geometry optimization. To augment the results by the B3LYP method, the same properties are calculated by the CCSD(T) method with the aug-cc-pVTZ basis set.

The geometries and vibrational properties of BCl_2^- and BCl_2 have been extensively studied by Warschkow and co-workers.[7] Jacox and co-workers also reported results[3] of quite extensive studies on BCl_2^+. Their best results using the CCSD(T) and B3LYP methods are also included in Table 1 for comparison. Though the previous work[4] by using the CCSD(T) method with an effective-core-potential reports the geometries and vibrational properties of BCl_2^- as well as BCl_2^+ and BCl_2, the results are

TABLE 2: The Calculated Results for $AlCl_2$ Systems. All Symbols Have the Same Meaning as Those in Table 1

method	R_e	∠	μ	$\nu_1(I_1)$	$\nu_2(I_2)$	$\nu_3(I_3)$
$AlCl_2^+(X\Sigma_g^{1+})$						
MP2(full)/6-31G*)[a]	1.997	180				
CCSD(T)/aug-cc-pVTZ	2.015	180	0	426(0)	136(98)	799(150)
B3LYP/aug-cc-pVTZ	2.011	180	0	419(0)	138(90)	790(151)
B3LYP/aug-cc-pVQZ	2.005	180	0	421(9)	133(90)	791(154)
$AlCl_2(\tilde{X}^2A_1)$						
(MP2(full)/6-31G*)[a]	2.096	118.8				
CCSD(T)/aug-cc-pVTZ	2.117	118.9	1.57	458(47)	146(9)	573(169)
B3LYP/aug-cc-pVTZ	2.124	119.5	1.65	439(44)	141(7)	553(169)
B3LYP/aug-cc-pVQZ	2.116	119.4	1.61	442(45)	144(7)	555(170)
$AlCl_2^-(\tilde{X}^1A_1)$						
CCSD(T)/aug-cc-pVTZ	2.291	98.8	1.05	357(108)	141(0.1)	339(137)
B3LYP/aug-cc-pVTZ	2.317	100.1	0.72	317(140)	131(0.1)	332(105)
B3LYP/aug-cc-pVQZ	2.309	100.2	0.80	318(140)	132(0.1)	332(106)
$AlCl_2^-(\tilde{a}^3B_1)$						
CCSD(T)/aug-cc-pVTZ	2.219	112.5	1.78	387(60)	126(0.1)	538[b](112)
B3LYP/aug-cc-pVTZ	2.222	114.5	1.87	362(57)	122(0.3)	436(106)
B3LYP/aug-cc-pVQZ	2.212	114.3	2.11	363(65)	125(0.4)	440(100)

[a] The results by Petrie.[12] [b] This value may possibly be affected by symmetry breaking.

not included here for conciseness. On the other hand, the previous theoretical results for $AlCl_2$ systems are quite limited, and only one comparable study[12] reported so far is limited to the geometries of $AlCl_2^+$ and $AlCl_2$. The MP2(full)/6-31G* results[12] are included in Table 2 for comparison. The experimental values for these systems are quite limited, and only a few experimental numbers[3,5,6] for BCl_2^+ and BCl_2 are included in Table 1. Because the harmonic frequencies of the present work are calculated by using the most abundant isotopes, the experimental frequencies of chemicals consisted of ^{11}B and ^{35}Cl are given in Table 1. The experimental values for geometries and vibrational properties of BCl_2^-, $AlCl_2^+$, $AlCl_2$, and $AlCl_2^-$ have not yet been reported.

For the positive ions and the neutrals, the B3LYP and the CCSD(T) methods with the same aug-cc-pVTZ basis set produce almost the same optimized geometries and vibrational properties except for the stretch frequencies (ν_1 and ν_3) of BCl_2 and $AlCl_2$ where the frequencies calculated by the CCSD(T) method are 15−20 cm^{-1} higher than those of the B3LYP method. On the other hand, the results of the B3LYP/aug-cc-pVQZ basis are almost identical with those of the B3LYP/aug-cc-pVTZ method. The B3LYP/aug-cc-pVTZ results of this work are also almost identical to the B3LYP/cc-pVTZ results of the previous work[7] for BCl_2 and BCl_2^+. On the basis of this comparison, the corresponding results of the CCSD(T)/aug-cc-pVQZ method, even though they are not calculated in the present work, are expected to be close to those of the B3LYP/aug-cc-pVQZ method within 0.005 Å, 1.0°, and 10−20 cm^{-1}. The B3LYP/aug-cc-pVQZ results of this work, not only for BCl_2 and BCl_2^+ but also for $AlCl_2$ and $AlCl_2^+$, can be regarded as the converged values in the one- and the multiparticle basis spaces.

A clearly resolved vibronic progression with a spacing of 650 ± 30 cm^{-1} was observed in the dispersed emission from vacuum-UV excitation of BCl_3,[5] and the authors of the work suggested that the progression may be due to $2\nu_2$ in the ground or excited state of BCl_2^+. The calculated symmetric bending frequency, 326 cm^{-1}, is very close to the experimentally suggested value, 325 ± 15 cm^{-1}. The harmonic frequencies of the asymmetric stretch of BCl_2^+ and BCl_2, calculated by the CCSD(T)/aug-cc-pVTZ method, are about 15−20 cm^{-1} higher than the experimental absorption frequencies. Considering some anharmonicity in the vibration, the agreement between the calculated and the experimental results are quite good enough. By using the infrared spectra of Ar/BCl_3 with simultaneous proton radiolysis, Miller and Andrews[6] assigned the weak absorption peak at 731 cm^{-1} to the symmetric stretch of $^{11}BCl_2$. The value is about 30 and 50^{-1} higher than the calculated harmonic frequencies using CCSD(T)/aug-cc-pVTZ and B3LYP/aug-cc-pVQZ methods, respectively. Because there is no reason to assume negative anharmonicity, the assignment is a little questionable. According to the experimental works,[3,6] the absorption frequency of asymmetric stretch of BCl_2^+ and BCl_2 increases about 40−60 cm^{-1} upon the replacement of the ^{11}B nucleus with the ^{10}B isotope. Accepting the high accuracy of the present calculations and assuming the similar isotope dependence in symmetric stretch, the weak absorption peak at 731 cm^{-1} can be assigned to $^{10}BCl_2$ rather than $^{11}BCl_2$. This argument may be resolved by more careful examination of the experimental spectrum.

For the lowest singlet($\tilde{X}^1A_1$) and triplet($\tilde{a}^3B_1$) states of the negative ions, the differences between the geometries calculated using the B3LYP/aug-cc-pVTZ method and those with the CCSD(T)/aug-cc-pVTZ method are a little larger than the corresponding differences for the positive ions and neutrals. The differences are about 0.005 Å in bond lengths and 1.0° in angles except for the bond length of the singlet state of $AlCl_2^-$ and the bond angle of the triplet state of $AlCl_2^-$, where the differences are 0.026 Å and 2.0°, respectively. The difference in vibrational frequencies of the two calculations are less than 10 cm^{-1} for the bending (ν_2), but about 20−40 cm^{-1} for stretches (ν_1 and ν_3) except the asymmetric stretch (ν_3) of $^3B_1$ of $AlCl_2^-$, for which the difference is as large as 100 cm^{-1}. There may possibly be some symmetry-breaking effect in ν_3 of the $\tilde{a}^3B_1$ state of BCl_2^- and $AlCl_2^-$, which is not explored in this work. The neglect of the core correlations in the present CCSD(T) calculations for geometries and vibrational properties, which was estimated to be about ±0.003 Å in bond length, ±0.3° in angles, and 1−2% of the calculated vibrational frequencies,[17] could be one part of the reasons for the differences. The remaining differences could be regarded as the intrinsic difference between the two correlation methods.

In spite of these small differences between results with the B3LYP and the CCSD(T) methods, the values in Tables 1 and 2 are expected to be reliable and predictive enough for subsequent experimental and theoretical studies on these negative species.

When the geometries, dipole moments, and vibrational properties of BCl_2^+, BCl_2, and BCl_2^- are compared with those

TABLE 3: Total Energy (E_{tot}) of Neutral, the Adiabatic Ionization Energy (AIE) of the Positive Ion, and the Adiabatic Electron Affinities of the Singlet (AEA_1) and the Triplet (AEA_3) States of Negative Ions. The Vertical Ionization Energies and the Vertical Electron Detachment Energies Are Given in Parentheses. All Values Are in eV Except the Total Energies in hartrees

	BCl_2 system				$AlCl_2$ system			
method	E[a]	AIE	AEA_1 (AIE_1^-)	AEA_3 (AIE_3^-)	E[b]	AIE	AEA_1 (AIE_1^-)	AEA_3 (AIE_3^-)
G1	−4.275 286	7.23	1.52	0.12	−1.588 895	7.79	2.44	0.39
G2	−4.274 537	7.25	1.47	0.13	−1.585 244	7.75[c]	2.42	0.40
CBS-4	−4.283 264	7.30	1.14	0.13	−1.594 250	7.76	2.25	0.43
CBS-Q	−4.288 760	7.30	1.47	0.22	−1.604 454	7.84	2.39	0.44
Other		7.33[d]						
B3LYP-DFT								
aug-cc-pVDZ	−5.297 531	7.57	1.48	0.32	−2.988 277	8.11	2.59	0.57
aug-cc-pVTZ	−5.331 804	7.44	1.38	0.27	−3.031 469	7.98	2.43	0.49
aug-cc-pVQZ	−5.341 082	7.43 (8.84)[e]	1.36 (2.16)[f]	0.26 (0.50)[f]	−3.043 824	7.98 (8.89)[e]	2.39 (2.92)[f]	0.47 (0.59)[f]
aug-cc-pV5Z[g]	−5.348 542	7.41	1.35	0.27	−3.051 987	7.96	2.38	0.47
CCSD(T)[h]								
aug-cc-pVDZ	−4.069 234	7.35	1.44	0.19	−1.419 268	7.89	2.48	0.54
aug-cc-pVTZ	−4.262 092	7.34 (8.78)[e]	1.42 (2.24)[f]	0.20 (0.46)[f]	−1.577 795	7.83 (8.80)[e]	2.38 (2.89)[f]	0.48 (0.63)[f]
aug-cc-pVQZ[i]	−4.309 029	7.39	1.45	0.23	−1.627 205	7.85	2.37	0.47
exptl		7.2,7.52[j]				7.82[k]		

[a] The total energy of $BCl_2(X^2A_1) = E - 940$. [b] The total energy of $AlCl_2(X^2A_1) = E - 1160$. [c] Petri reports the same value.[12] [d] By using the calculated Gibbs free energy at 298 K[7] with the G2 theory. [e] The vertical ionization energy (VIE). [f] The vertical electron detachment energy (VEDE), i.e., the vertical ionization energy of negative ion (VIE^-). [g] The aug-cc-pV5Z energy at the aug-cc-pVQZ geometry. [h] The 22 and 30 core electrons of BCl_2 and $AlCl_2$ systems, respectively, are frozen in the coupled-cluster correlation calculations. [i] The aug-cc-pVQZ energy at the aug-cc-pVTZ geometry. [j] Koski et al.[22] gave 7.2 eV, while Dibeler and Walker[23] obtained 7.52 eV. [k] Calculated by using the experimental (0 K) enthalpy of formation taken from JANAF compendium.[24]

of the aluminum analogs, it can be seen that, by replacing the B atom with Al atom, the bond lengths increase by about 0.4 Å and the bond angles of C_{2v} structure decrease about 4−6°. While harmonic frequencies of all vibration modes and IR intensities of asymmetric stretch mode decrease substantially by the replacement, IR intensities of the symmetric stretch mode doubled, but are still rather small. It is also interesting to see that the dipole moment (μ) of the triplet states are very similar in BCl_2^- and $AlCl_2^-$, whereas the μ of the singlet state decreases substantially and the μ of the neutral species increase greatly by replacing B with Al.

Ionization Energies and Electron Affinities. Adiabatic ionization energies (AIE) and adiabatic electron affinities for the lowest singlet and triplet states (AEA_1 and AEA_3) are calculated by the G1, G2, CBS-4, and CBS-Q methods, as shown in Table 3. The B3LYP method using the aug-cc-pVDZ, aug-cc-pVTZ, and aug-cc-pVQZ basis sets as well as the CCSD(T) method using the aug-cc-pVDZ and aug-cc-pVTZ basis sets are also used in the calculations of AIEs and AEAs. In addition, single-point calculations using the B3LYP/aug-cc-pV5Z and the CCSD(T)/aug-cc-pVQZ method are performed at the geometries obtained using the B3LYP/aug-cc-pVQZ and the CCSD(T)/aug-cc-pVTZ methods, respectively. The vertical ionization energies and the vertical electron detachment energies are calculated only by the B3LYP/aug-cc-pVQZ and the CCSD(T)/aug-cc-pVTZ methods. The zero-point energies (ZPEs) without using any scale factor, i.e., within the harmonic approximation, are corrected for in the calculation of these energetic properties.

The results in Table 3 indicate that our best estimates, the results by B3LYP/aug-cc-pV5Z and CCSD(T)/aug-cc-pVQZ methods, for energetic separations have attained basis-set limits of each correlation method within a few hundredths of an eV. For the energetic properties in Table 3, the deviations among results obtained by the G2, CBS-Q, B3LYP/aug-cc-pV5Z, and CCSD(T)/aug-cc-pVQZ methods are estimated to be about 0.05 eV. The energetic values of CBS-Q are a little closer to those from the CCSD(T)/aug-cc-pVQZ method than those from B3LYP/aug-cc-pV5Z.

The AIE of BCl_2 was calculated to be 7.25 eV at 0 K and 7.33 eV at 298 K by using the calculated Gibbs free energies of BCl_2 and BCl_2^+,[7] which are comparable to the earlier experimental value, 7.2 eV.[22] On the other hand, we calculate the AIE to be 7.30 eV by the CBS-4 and the CBS-Q methods and about 7.40 eV by the B3LYP/aug-cc-pV5Z and the CCSD(T)/aug-cc-pVQZ methods, which are closer to the latest experimental value, 7.52 eV.[23]

The calculated AIE of $AlCl_2$ by the G2 and the B3LYP/aug-cc-pV5Z methods, 7.75 eV and 7.96 eV, respectively, are within the error bound of the experimental value, 7.82 ± 0.98 eV.[24] The results by using the CBS-Q and the CCSD(T)/aug-cc-pVQZ methods, 7.84 and 7.85 eV, respectively, are more close to the experimental value. We expect that our results are reliable at least within 0.1 eV.

It turns out that the lowest singlet and triplet states of BCl_2^- and $AlCl_2^-$ are stable relative to their neutrals. The adiabatic electron affinity (AEA) and the ZPE of each species are as follows: $AEA_1 = 1.40$ eV and ZPE = 0.07 eV for BCl_2^- ($\tilde{X}1^{A}{}_1$), $AEA_3 = 0.25$ eV and ZPE = 0.09 eV for BCl_2^- ($\tilde{a}^3B_1$), $AEA_1 = 2.37$ eV and ZPE = 0.05 eV for $AlCl_2^-$ ($\tilde{X}^1A_1$), and $AEA_3 = 0.46$ eV and ZPE = 0.06 eV for $AlCl_2^-$ ($\tilde{a}^3B_1$). Though the AEA of triplet state of BCl_2^- is as small as 0.25 eV, it can be compared to the AEA of BCl_3^-, 0.33 ± 0.2 eV which was determined by the charge transfer method[25] and supported by previous calculations.[4] As a result, there are ample possibilities that such negative species could be formed by collision with secondary electrons of low energy and could play an important role in the radio frequency plasma etching processes. Though the possibility of the stable BCl_2^- was mentioned qualitatively in a previous publication,[4] the present work is the first quantitative prediction for the stability of these negative ions. The geometries and vibrational properties of the lowest singlet and triplet states of BCl_2^- and $AlCl_2^-$ in Tables 1 and 2, respectively, are expected to be useful in the near future. The role of these negative species in the overall plasma processes may be an open question.

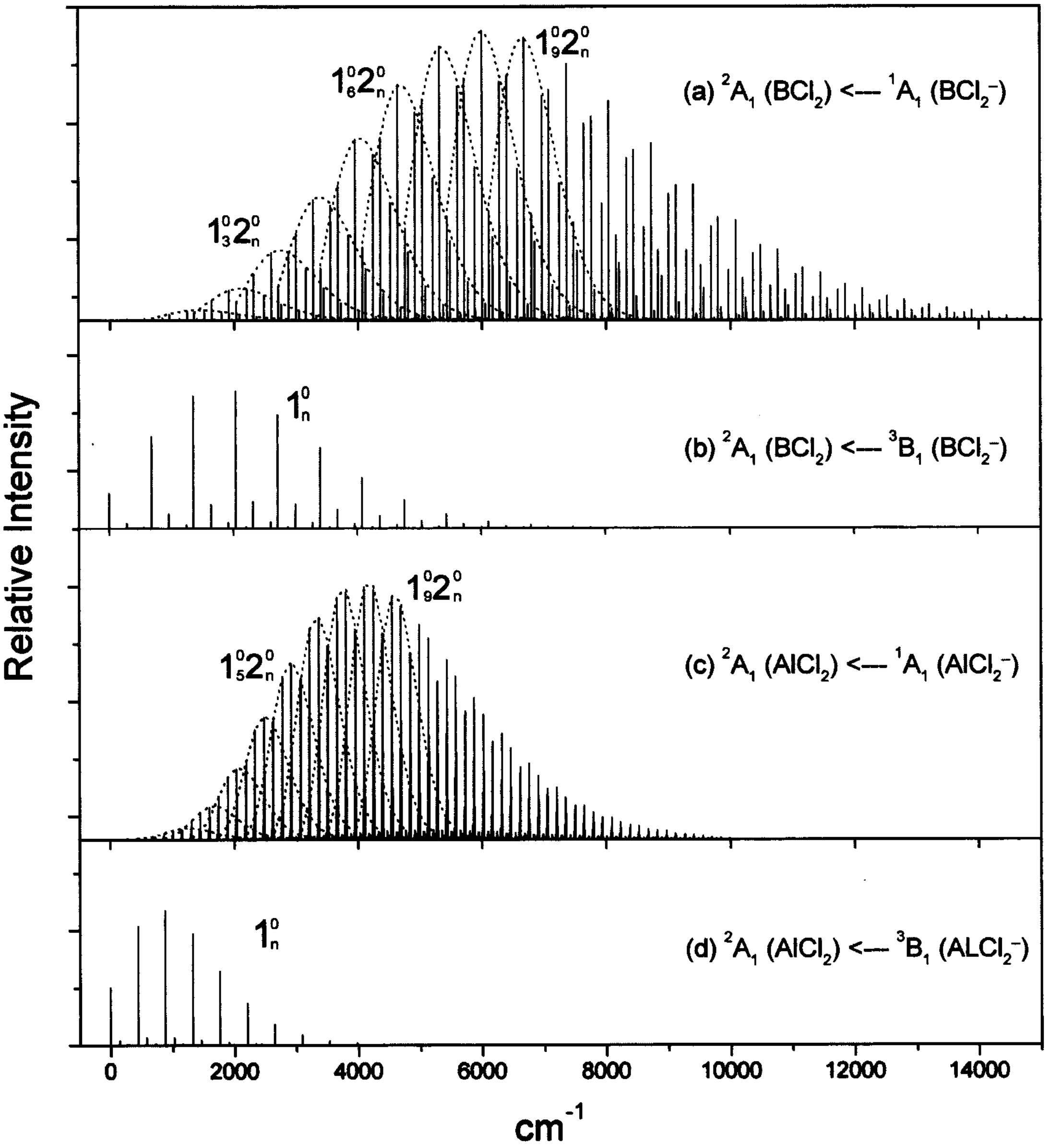

Figure 1. The simulated photoelectron spectra for (a) $\tilde{X}^2A_1(BCl_2) \leftarrow \tilde{X}^1A_1(BCl_2^-)$, (b) $\tilde{X}^2A_1(BCl_2) \leftarrow \tilde{a}^3B_1(BCl_2^-)$, (c) $\tilde{X}^2A_1(AlCl_2) \leftarrow \tilde{X}^1A_1(AlCl_2^-)$, and (d) $\tilde{X}^2A_1(AlCl_2) \leftarrow \tilde{a}^3B_1(AlCl_2^-)$ transitions.

Photoelectron Spectra of Negative Ions. Because we suggest the stability of negative ions, the photoelectron spectra of singlet and triplet states of BCl_2^- and $AlCl_2^-$ are simulated by calculating Franck−Condon factors (FCFs), and the simulated photoelectron spectra are shown in Figure 1. The FCFs are calculated by using the B3LYP/aug-cc-pVQZ structures and frequencies, and all possible transitions are included in Figure 1 with arbitrary relative intensities normalized with respect to the 0^0_0 band of each spectrum.

From the overall spectral envelopes, we can see that the simulated spectra are similar for BCl_2^- and $AlCl_2^-$ while quite different between $^2A_1 \leftarrow {}^1A_1$ and $^2A_1 \leftarrow {}^3B_1$ photodetachments. The adiabatic electron affinity (AEA) and the vertical electron detachment energy (VEDE) in Table 3 can be regarded as the adiabatic ionization energy of negative ion (AIE$^-$) and the vertical ionization energy of negative ion (VIE$^-$), respectively. As can be seen from the table, AIE$_3^-$/VIE$_3^-$/(the difference between them) of triplet states are 0.26 eV/0.50 eV/(0.24 eV) and 0.47 eV/0.59 eV/(0.12 eV) for BCl_2^- and $AlCl_2^-$, respectively, while those of singlet states are 1.36 eV/2.16 eV/(0.80 eV) and 2.39 eV/2.92 eV/(0.53 eV). The differences between AIE$^-$ and VIE$^-$ are reflected in the different location of the overall maximum peaks of the four spectra in Figure 1, i.e., 0.80 eV vs ~6000 cm^{-1}(BCl_2^-,$\tilde{X}^1A_1$), 0.24 eV vs ~1700 cm^{-1} (BCl_2^-,$\tilde{a}^3B_1$), 0.53 eV vs ~4200 cm^{-1}($AlCl_2^-$,$\tilde{X}^1A_1$), and 0.12 eV vs ~900 cm^{-1}($AlCl_2^-$,$\tilde{a}^3B_1$). From the bond lengths and angles in Tables 1 and 2, we can also see that the changes in geometry for $^2A_1 \leftarrow {}^1A_1$ are much larger than those in $^2A_1 \leftarrow {}^3B_1$.

For $^2A_1 \leftarrow {}^1A_1$ detachments, the changes in bond angle and bending frequency are +21.5 degrees/+40 cm^{-1} and +19.2 degrees/+12 cm^{-1} in BCl_2^- and $AlCl_2^-$, respectively, and the changes in bond length and symmetric stretch frequency are −0.197 Å/+282 cm^{-1} and −0.193 Å/+124 cm^{-1} in BCl_2^- and $AlCl_2^-$, respectively. The larger rotation of the normal coordinates in the $^2A_1 \leftarrow {}^1A_1$ transition is responsible for the complicated series of combination bands of (a) and (c) of Figure 1, which is a typical demonstration of the Duschinsky effect.[26] The calculated FCFs reveal that there are many combinations between symmetric stretch and bending modes in the $^2A_1 \leftarrow {}^1A_1$ electron detachment process. Some series of the prominent combination bands are connected by dotted lines in Figure 1a and c to show that overall spectral envelopes are determined by the combinations between ν_1 and ν_2 modes. Further analysis in detail for other combination bands is not attempted here because they are not expected to offer any additional insight.

For the $^2A_1 \leftarrow {}^3B_1$ detachments, on the other hand, the changes in bond angle and bending frequency are only +5.5 degrees/+56 cm^{-1} and +5.0 degrees/+19 cm^{-1} in BCl_2^- and $AlCl_2^-$, respectively, and the changes in bond length and symmetric stretch frequency are −0.114 Å/+136 cm^{-1} and −0.096 Å/+73 cm^{-1} in BCl_2^- and $AlCl_2^-$, respectively. In this case, only a single vibrational progression turns out to have a detectable intensity. The intervals in the vibrational progressions, 680 cm^{-1} in Figure 1b and 442 cm^{-1} in Figure 1d, correspond to the symmetric stretch frequency of BCl_2 and $AlCl_2$, respectively. The fewer vibration progressions in Figure 1d than in b reflects the smaller changes in geometry and vibrational frequencies during the electron detachment.

Conclusions

By employing two complementary high level correlation methods, the B3LYP method[8] and the CCSD(T) method,[9] in conjunction with the aug-cc-pVXZ basis sets[18] up to QZ and 5Z, accurate and predictive results for the structures, dipole moments, vibrational properties, and energetic properties (IE and EA) of positive ($X\Sigma_g^{1+}$), neutral ($\tilde{X}^2A_1$), and negative ($\tilde{X}^1A_1$ and $\tilde{a}^3B_1$) states of BCl_2^- and $AlCl_2^-$ have been obtained and should prove useful for future experimental work.

It is shown that both the $\tilde{X}^1A_1$ and $\tilde{a}^3B_1$ states of negative ions, which have never been studied experimentally but we expected to be involved in plasma etching processes, are stable with electron affinities of $AEA_1 = 1.40$ eV/$AEA_3 = 0.25$ eV and $AEA_1 = 2.37$ eV/$AEA_3 = 0.46$ eV for singlet/triplet states of BCl_2^- and $AlCl_2^-$, respectively.

The photoelectron spectra for the singlet and triplet states of BCl_2^- turn out to be very similar to the $AlCl_2^-$ analogs. While the photoelectron spectra for $\tilde{X}^2A_1(MCl_2) \leftarrow \tilde{X}^1A_1(MCl_2^-)$, M = B and Al, have a complicated structure dominated by the combination between the symmetric stretch and bending modes, those for $\tilde{X}^2A_1(MCl_2) \leftarrow \tilde{a}^3B_1(MCl_2^-)$, M = B and Al, have only one vibrational progression of the symmetric stretch mode.

Acknowledgment. The authors are grateful to Professor Rodney J. Bartlett for the ACES-II program, and to Dr. T. Momose for the FCF program. This work was supported by the Korea Science and Engineering Foundation under Grant KOSEF-981-0306-031-2. K.K.B also appreciates the Ministry of Education, Science, Sport, and Culture, Japan, for supporting his stay in IMS. Computations in the present work are carried out by using the CRAY C90 of the SERI Supercomputer center and the computers in the computer center of IMS.

References and Notes

(1) Lee, J. W.; Hong, J.; Lambers, E. S.; Abernathy, C. R.; Pearton, S. J.; Hobson, W. S.; Ren, F. *Plasma Chem. Plasma Proc.* **1997**, *17*, 155.

(2) Lister, G. G. *Vacuum* **1994**, *45*, 525, and references therein.

(3) Jacox, M. E.; Irikura, K. K.; Thompson, W. E. *J. Chem. Phys.* **1996**, *104*, 8871.

(4) Baeck, K. K.; Bartlett, R. J. *J. Chem. Phys.* **1997**, *106*, 4604.

(5) Biehl, H.; Creasey, J. C.; Smith, D. M.; Tuckett, R. P.; Yoxall, K. R.; Baumgartel, H.; Jochims, H. W.; Rockland, U. *J. Chem. Soc., Faraday Trans.* **1995**, *91*, 3073.

(6) Miller, J. H.; Andrews, L. *J. Am. Chem. Soc.* **1980**, *102*, 4900.

(7) Warschkow, O.; Lee, E. P. F.; Wright, T. G. *J. Chem. Soc., Faraday Trans.* **1997**, *93*, 53.

(8) (a) Becke, A. D. *J. Chem. Phys.* **1993**, *98*, 5648. (b) Lee, C.; Yang, W.; Parr, R. G. *Phys. Rev. B* **1988**, *37*, 785.

(9) Bartlett, R. J.; Watts, J. D.; Kucharski, S. A.; Noga, J. *Chem. Phys. Lett.* **1990**, *165*, 513.

(10) Pearton, S. J.; Hobson, W. S.; Albernathy, C. R.; Ren, F.; Fullowan, T. R.; Katz, A.; Perley, A. P. *Plasma Chem. Plasma Proc.* **1993**, *13*, 311.

(11) Köppe, R.; Kasai, P. H. *J. Am. Chem. Soc.* **1996**, *118*, 135.

(12) Petrie, S. *J. Phys. Chem.* **1998**, *102*, 7828.

(13) Frisch, M. J.; Trucks, G. W.; Schlegel, H. B.; Gill, P. M. W.; Johnson, B. G.; Robb, M. A.; Cheeseman, J. R.; Keith, T.; Petersson, G. A.; Montgomery, J. A.; Raghavachari, K.; Al-Laham, M. A.; Zakrzewski, V. G.; Ortiz, J. V.; Foresman, J. B.; Cioslowski, J.; Stefanov, B. B.; Nanayakkara, A.; Challacombe, M.; Peng, C. Y.; Ayala, P. Y.; Chen, W.; Wong, M. W.; Andres, J. L.; Replogle, E. S.; Gomperts, R.; Martin, R. L.; Fox, D. J.; Binkley, J. S.; Defrees, D. J.; Baker, J.; Stewart, J. P.; Head-Gordon, M.; Gonzalez, C.; Pople, J. A. GAUSSIAN94; Gaussian, Inc.: Pittsburgh, PA, 1995.

(14) (a) Curtiss, L. A.; Jones, C.; Trucks, G. W.; Raghavachari, K.; Pople, J. A. *J. Chem. Phys.* **1990**, *93*, 2537. (b) Curtiss, L. A.; Raghavachari, K.; Trucks, G. W.; Pople, J. A. *J. Chem. Phys.* **1991,** *94*, 7221.

(15) Petersson, G. A.; Tensfeldt, T. G.; Montgomery, J. A., Jr. *J. Chem. Phys.* **1991**, *94*, 6091.

(16) Quantum Theory Project, Stanton, J. F.; Gauss, J.; Watts, J. D.; Nooijen, M.; Oliphant, N.; Perera, S. A.; Szalay, P. G.; Lauderdale, W. J.; Gwaltney, S. R.; Beck, S.; Balková, A.; Bernholdt, D. E.; Baeck, K. K.; Rozyczko, P.; Sekino, H.; Hober, C.; Bartlett, R. J. Advanced Concepts in Electronic Structure Theory (ACES-II); University of Florida, Gainesville. Integral packages included are VMOL (Almlöf, J.; Taylor, P. R., VPROPS (Taylor, P.), ABACUS (Helgaker, T.; Jensen, H. J. Aa.; Jorgensen P.; Olsen, J.; Taylor, P. R.).

(17) Baeck, K. K.; Watts, J. D.; Bartlett, R. J. *J. Chem. Phys.* **1997**, *107*, 3853.

(18) (a) Woon, D. E.; Dunning, T. H., Jr. *J. Chem. Phys.* **1993**, *98*, 1358. (b) Dunning, T. H., Jr. *J. Chem. Phys.* **1989**, *90*, 1007.

(19) (a) Davidson, E. R. *Chem. Phys. Lett.* **1996**, *260*, 514. (b) Hashimoto, T.; Hirao, K.; Tatewaki, H. *Chem. Phys. Lett.* **1995**, *243*, 190.

(20) Sharp, T. E.; Rosenstock, H. M. *J. Chem. Phys.* **1964**, *41*, 3453.

(21) Yamaguchi, M.; Momose, T.; Small, G. J. *J. Chem. Phys.* **1990**, *93*, 4211.

(22) Koski, W. S.; Kaufman, J. J.; Puchucki, C. F. *J. Am. Chem. Soc.* **1959**, *81*, 1326.

(23) Dibeler, V. H.; Walker, J. A. *Inorg. Chem.* **1969**, *8*, 50. *7*, 551.

(24) Chase, M. W., Jr.; Davies, C. A.; Downey, J. R., Jr.; Frurip, D. J.; McDonald, R. A.; Syverup, A. N. *J. Phys. Chem. Ref. Data, Suppl.* **1985**, *14* (1).

(25) Rothe, E. W.; Mathur, B. P.; Reck, G. P. *Inorg. Chem.* **1980**, *19*, 829.

(26) Duschinsky, F. *Acta Physicochim. URSS.* **1937**, *7*, 551.